Eur. Phys. J. B **19**, 157–162 (2001)

THE EUROPEAN PHYSICAL JOURNAL B

EDP Sciences

Experimental characterization of intermittency regimes in the Couette-Taylor system

A. Goharzadeh and I. Mutabazi[a]

Laboratoire de Mécanique, Université du Havre, 25 rue Philippe Lebon, BP 540, 76058 Le Havre Cedex, France

Received 15 December 1999 and Received in final form 19 October 2000

Abstract. We investigate experimentally the properties of spatio-temporal intermittency states (turbulent bursts and spiral turbulence) in the counter-rotating Couette-Taylor system. The mean turbulent fraction increases continuously from turbulent bursts to spiral turbulence and depends on the angular velocity of both cylinders. The axial velocity of turbulent spirals, which depends only on the outer cylinder, is smaller than the azimuthal component.

PACS. 47.20.Ky Nonlinearity (including bifurcation theory) – 47.27.Cn Transition to turbulence

1 Introduction

Spatio-temporal intermittency (STI) represents an intriguing feature of the transition to turbulence: it is a fluctuating mixture of ordered laminar domains and incoherent turbulent patches in space and time for the same value of the control parameter. This phenomenon involves spatial as well as temporal degrees of freedom of the system. This transition has been observed in shear flows such as boundary layer flow [1], pipe flow [2], plane Poiseuille flow [3,4], the counter-rotating Couette-Taylor system [5–7] and the Taylor-Dean system [8]. It has also been observed in Rayleigh-Bénard convection for large values of temperature gradients [9,10] and in array of 2d vortices forced electromagnetically [11]. The coexistence of two different dynamical states, of particular interest in hydrodynamic systems, has also been evidenced in numerical simulations of coupled map lattices [12], in nonlinear partial differential equations such as the damped Kuramoto-Sivashinsky equation [13] or the complex Ginzburg-Landau equation [14–16] and in probabilistic cellular automata [17]. The coexistence of two different stable states for the same values of the control parameter, can be seen as consequence of a subcritical bifurcation and is described by a fifth order Landau equation [18].

The spatio-temporal intermittency observed in the Couette-Taylor system reveals special features: turbulent bursts occur erratically in time and space in the laminar phase of interpenetrating spiral, while a turbulent spiral coexists with a spiral of laminar base flow [5, 6] in a wide range of values of the control parameter. The transition to turbulent bursts from interpenetrating spiral pattern has been investigated numerically by Coughlin and Marcus [19] and experimentally by Colovas and Andereck [20] who have measured their turbulent fraction and the statistical properties of laminar domains as function of the control parameter. The latter noticed the lack of a regime of exponential decay of laminar length which would correspond to the supercritical transition analogous to the contamination phase of the directed percolation according to Pomeau's conjecture [18]. In fact, above a given value of the control parameter, the turbulent bursts merge to form a turbulent spiral. The resulting flow state called *spiral turbulence* is characterized by coexistence of stable turbulent and laminar spirals for finite range of the control parameter. Hegseth *et al.* [21] have investigated experimentally the kinematics of a turbulent spiral and explained some of its properties (pitch and azimuthal velocity) using a phase dynamics equation. Later on, Hayot and Pomeau [22] explained the stable coexistence of turbulent spiral together with a laminar one, using a quintic Ginzburg-Landau equation, in which they included a nonlocal term that serves to prevent the turbulent domain expansion.

In this paper, we report new experimental results of the transition from interpenetrating spirals to turbulent bursts and focus our attention on the properties of a turbulent spiral that, to the best of our knowledge, have not been reported before. We have measured the turbulent fraction of both regimes, the average duration of turbulent bursts, the period, the axial velocity and the width of turbulent spirals. In next section, we describe the experimental setup and procedures, the results are presented

[a] e-mail: mutabazi@univ-lehavre.fr

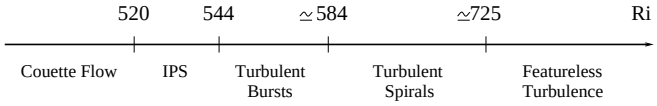

Fig. 1. Diagram of states observed in counter-rotating Couette-Taylor system for $Ro = -1375$. The terminology is borrowed from Andereck *et al.* [5].

in Section 3 and their discussion in Section 4. The last section contains concluding remarks.

2 Experimental setup and procedures

The Couette-Taylor configuration used in our experiments consists of two coaxial horizontal counter-rotating cylinders. The inner cylinder is made of black Delrin with a radius $a = 4.459\,\text{cm}$. The outer cylinder is made of transparent Plexiglas with a radius $b = 5.050\,\text{cm}$. The gap between the cylinders is $d = b - a = 0.591\,\text{cm}$ over a length $L = 27.5\,\text{cm}$. Hence the system has a radius ratio $\eta = a/b = 0.88$, and an aspect ratio $\Gamma = L/d = 46$. Both cylinders are driven independently in opposite direction by two DC servomotor. Thus the control parameters of the Couette-Taylor system are the Reynolds numbers defined for the inner and outer cylinders respectively: $R_i = \Omega_i ad/\nu$ and $R_o = \Omega_o bd/\nu$, where Ω_i and Ω_o are angular frequencies of inner and outer cylinder respectively and ν the kinematic viscosity of the fluid. We used distilled water ($\nu = 10^{-2}\,\text{cm}^2/\text{s}$ at $T = 21\ ^\circ\text{C}$) to which we added 2% Kalliroscope AQ1000 for visualization. With a light from a fluorescent tube, the flow was visualized on the front side. To obtain spatial information about the flow dynamics, a linear 1024-pixel charge coupled device (CCD) array records the intensity distribution $I(x)$ of the light reflected by Kalliroscope flakes from a line along the axis at the middle of cylinders. The recorded length is from 20 to 25 cm in the central part of the system, corresponding to a spatial resolution of 41 to 51 pixels/cm. The intensity is sampled in 256 values, displayed in grey levels at regular time intervals along time axis to produce space-time diagrams $I(x,t)$ of the pattern.

3 Results

We characterize the weak turbulent states observed in the counter-rotating Couette-Taylor system for fixed outer cylinder rotation (Ro =const.) and varying Ri in the state diagram of Andereck *et al.* [5] (Fig. 1). A centrifugal instability of the base flow induces a supercritical Hopf bifurcation that gives rise to interpenetrating spirals above Ri^+ which varies with Ro (Fig. 1: for $Ro = -1375, Ri^+ = 520$). Interpenetrating spirals can be seen as waves propagating in opposite directions and which interfere (Fig. 2) in space. The interpenetrating spirals are stable in a small range of values of Ri and above Ri^*, they pertain a secondary subcritical instability (*i.e.* they become unstable to finite amplitude perturbations) which manifests itself in form of turbulent bursts occurring irregularly in time at different positions of the flow (Fig. 3). The occurrence of a turbulent burst induces a dissymmetry in the pattern, the intensity of interpenetrating spirals decreases in the wake of a turbulent burst. The average number per unit time, the lifetime and size of the turbulent bursts increase with Ri. As the inner cylinder rotation rate increases, the turbulent bursts acquire an axial velocity component, smaller than the azimuthal velocity component, and hence they are inclined with respect to the cylinder axis (Fig. 4). When the length of the burst becomes comparable with the half perimeter of the cylinder, bursts connect to form a turbulent spiral. The pattern is then composed of two alternating turbulent and laminar spirals (Fig. 5). The turbulent spiral coexists with the laminar spiral for a long time without annihilating each other in a wide range of the values of the control parameter (Fig. 1). In that range of values of Ri, the axial width of the turbulent spiral remains constant. Moreover, the turbulent spiral has no preferred direction of propagation, it may have right or left helicity. In fact, we have determined the probability of occurrence of left or right helicity over 120 runs and found $50\% \pm 4\%$ for each case. For some runs (especially with a rapid increase in Ri), we have observed transient turbulent spirals of both left and right helicity separated by a defect which disappeared after a few minutes giving rise to a turbulent spiral of a given helicity. For very large values of Ri ($Ri > 725$ for $Ro = -1375$), the turbulent spiral spreads while the laminar spiral decays and the flow becomes completely turbulent (featureless turbulence).

In order to quantitatively characterize the observed states, we have measured, from the space-time diagrams, the lifetime, the axial length and the frequency (number per unit time) of turbulent states. We have binarized the space-time diagrams as follows: after a choice of a cutoff criterion, the laminar phase is set to 0 (white) and the turbulent state to 1 (black). Then we have determined the mean turbulent fraction as the total area of turbulent region to the total measured area of the space-time diagram. The mean turbulent fraction is zero in the laminar state and reaches its maximum value (1) in the completely turbulent state. For weak values of ϵ ($\epsilon < 0.05$), the turbulent fraction for bursts is an increasing function of Ri and its slope depends on the value of Ro (Fig. 6). With an increase of Ri, the turbulent bursts occur more frequently and grow in size until they connect each other to form a turbulent spiral ($0.05 < \epsilon < 0.2$). The fraction of the turbulent spiral is a linear function of Ri (the part of the curve in Fig. 6 for $\epsilon > 0.2$) and varies with Ro. The variation of the turbulent fraction of turbulent spiral with Ro has been determined for runs at fixed $Ri = 610, Ri = 670$ (Fig. 7); the difference between the two curves is due to the fact that the range of the values of Ro for which turbulent spirals are observed for $Ri = 670$ is larger than that for $Ri = 610$. The lifetime of turbulent bursts and turbulent spiral increases with ϵ. The frequency of turbulent spirals does not depend on ϵ. We have measured the average axial width l of the turbulent spiral and found that it is constant with respect to Ri (Fig. 8). The axial velocity

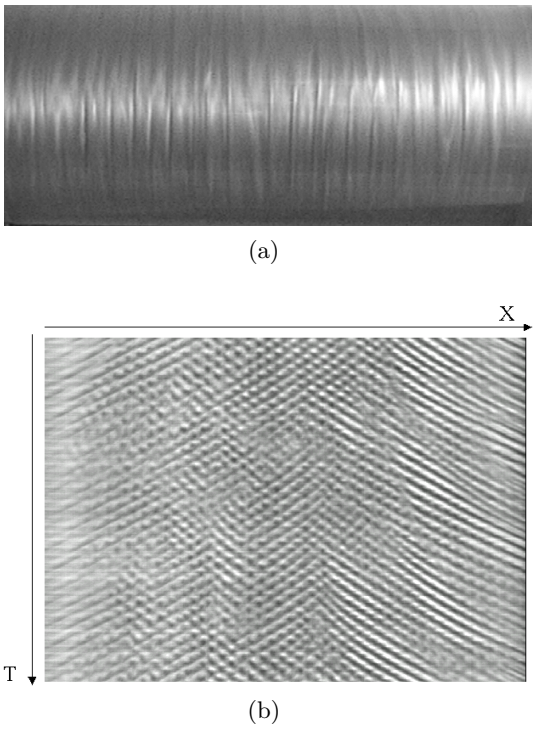

Fig. 2. (a) Picture and (b) spatio-temporal diagram of interpenetrating spiral near the onset $Ri^+ = 520$ for $Ro = -1375$. The corresponding wavenumber is $q = 1.44$ cm^{-1} and the frequency is $f = 0.707$ Hz.

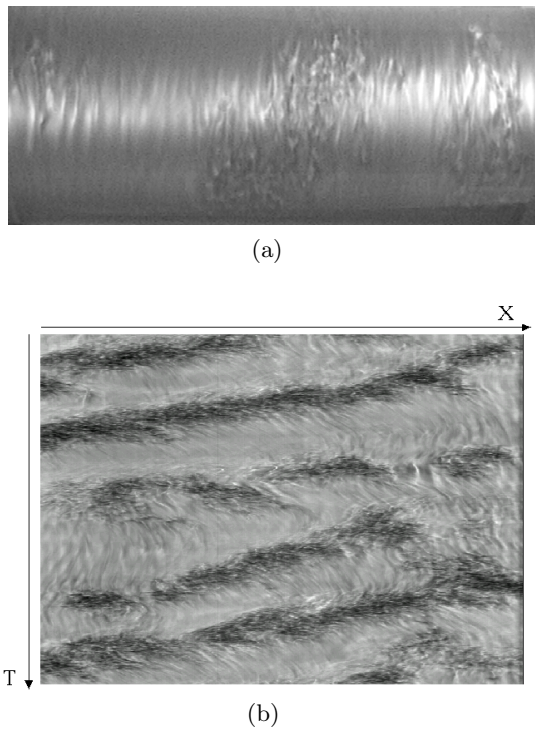

Fig. 4. (a) Picture and (b) spatio-temporal diagram of connecting turbulent bursts for $Ro = -1375, Ri = 580$.

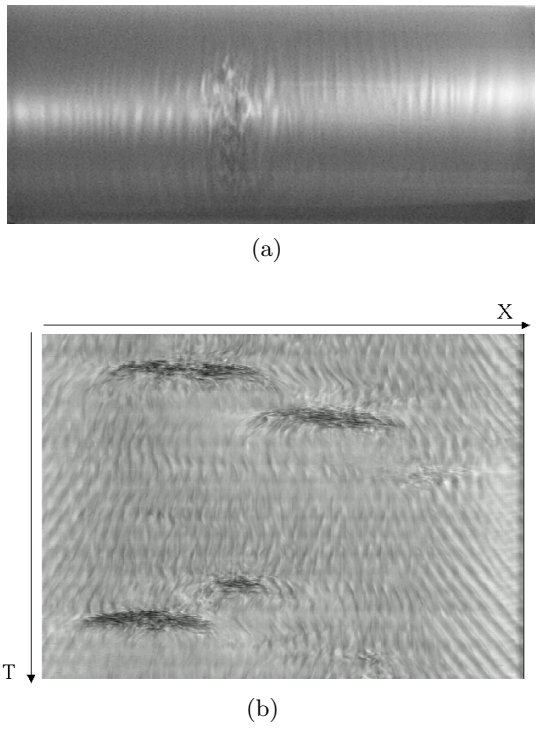

Fig. 3. (a) Picture and (b) spatio-temporal diagram of spontaneous nucleation of turbulent bursts for $Ro = -1375$, $Ri = 544$.

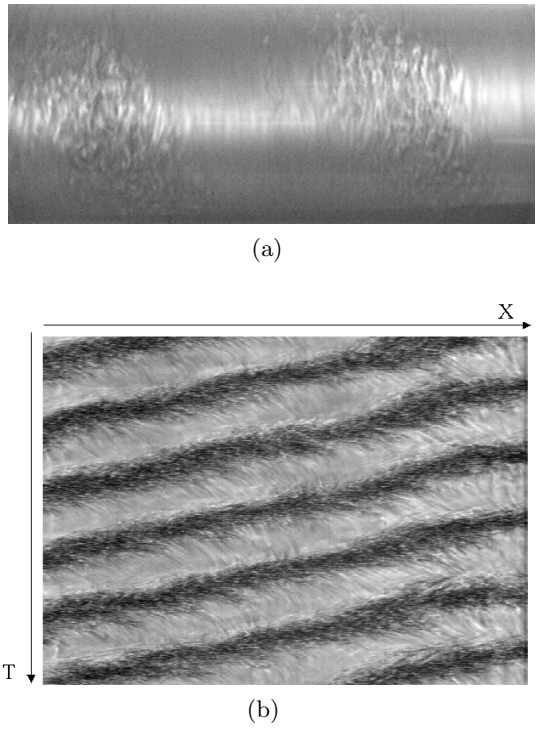

Fig. 5. (a) Picture and (b) spatio-temporal diagram of turbulent spiral for $Ro = -1375, Ri = 611$.

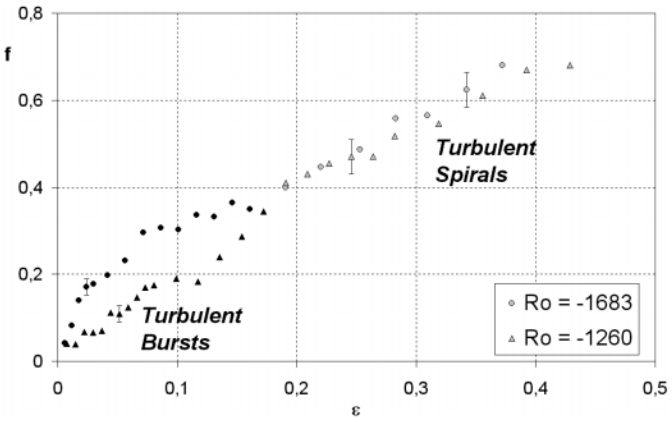

Fig. 6. Turbulent fraction of turbulent bursts and turbulent spirals *vs.* $\epsilon = \frac{Ri - Ri^*}{Ri^*}$.

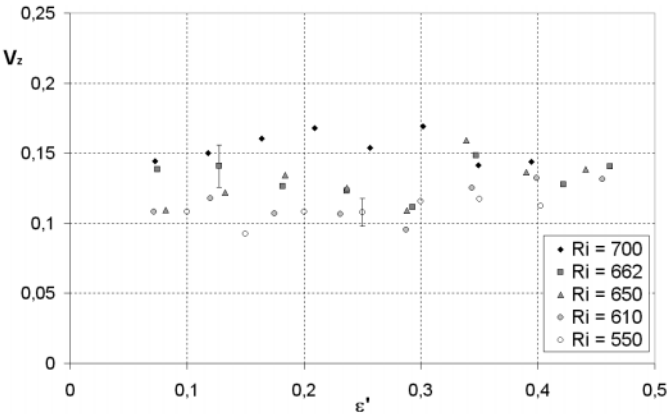

Fig. 9. Axial velocity of turbulent spirals in units of diffusion velocity $\Omega_o b$ as a function of $\epsilon^{'}$.

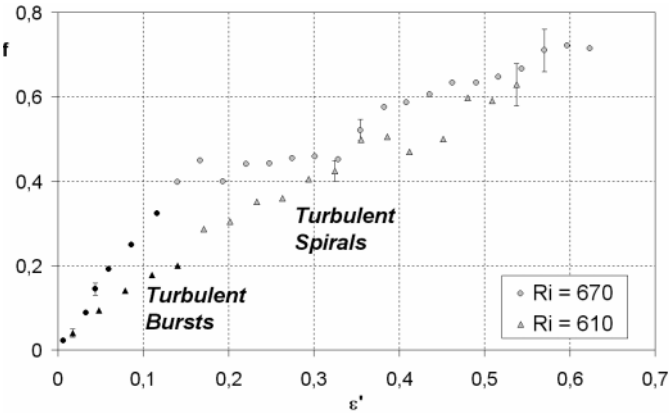

Fig. 7. Turbulent fraction of turbulent spirals as a function of $\epsilon^{'} = \frac{Ro - Ro_c}{Ro_c}$, where Ro_c is the critical value for which bursts occur for fixed value of Ri.

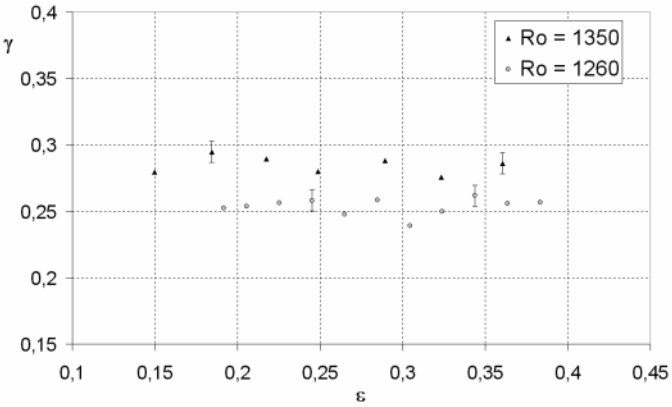

Fig. 8. Ratio γ of the average axial l width of turbulent spiral l to the total working length L of the flow system as function of ϵ for $Ro = -1260$ and $Ro = -1350$.

of turbulent spiral was obtained as the ratio of the axial length to the time duration of turbulent spiral, it increases with ϵ'(Fig. 9) for fixed value of Ri. We measured the inclination angle of turbulent spiral also called *pitch angle* and found that it varies from 21° to 40°. Using geometrical consideration, we have deduced from these values, an approximate value of the azimuthal velocity which was found to be at least 1.5 times larger than the axial velocity.

4 Discussion

The bursting phenomenon is governed by the space distribution of energy transferred from rotating cylinders to the interpenetrating spirals. In fact, we observed the disappearance of interpenetrating spirals in the wake of turbulent bursts as a consequence of the strong energy dissipation by the bursts. A similar behaviour has been observed in the Emmons turbulent spots occurring in boundary-layers over plane plates [1,23]. The generation of a new burst occurs not in the wake of previous one but either at the left or the right of this wake where less energy is dissipated. The turbulent fraction dependence on Ri for fixed Ro follows the same behaviour as that of Colovas and Andereck [20] for turbulent bursts. The strong dependence of turbulent fraction on Ri means that the inner cylinder is more responsible than the outer cylinder for the energy transfer to the fluctuations that dissipate in the turbulent regime. This is due to the centrifugal instability very active near the inner cylinder, so the growth rate of the finite amplitude perturbations generating the bursts is stratified in the radial direction. The turbulent fraction is correlated with the lifetime and size of turbulent domains in the space-time diagrams. In fact, the number, mean lifetime and size of turbulent bursts increase with the control parameter Ri, that is why the turbulent fraction f increases with Ri. The statistics of the laminar domains *versus* their width have been reported in [20].

No statistics on width of turbulent spiral can be achieved since the turbulent spiral has approximately constant axial width (Fig. 8).

The axial velocity of turbulent spiral is smaller than the azimuthal velocity, it is a linear function of Ro and it is independent of Ri in agreement with previous results [5]. This behaviour may be explained if one considers that the turbulent and laminar spirals form a spatio-temporal pattern with a selected wavelength (depending on the system aspect ratio) and drifting at the same velocity. The period of the turbulent spiral increases with Ri while that of laminar spiral decreases keeping constant the mean period of the turbulent-laminar pattern. This is why the fraction of turbulent spirals increases with Ri but their axial velocity remains constant. For fixed Ri, the period of turbulent-laminar spirals increases and since the average size is constant, the axial velocity of spirals increases with Ro. The behaviour of turbulent spiral is very sensitive to the boundary conditions imposed to the flow [24] and to the aspect ratio of the system [25].

According to numerical results of Coughlin *et al.* [19], the interpenetrating spirals are destabilized by an azimuthal traveling wave (induced by a secondary instability). A nonlinear stability analysis of the interpenetrating spirals [26] shows that azimuthal and axial mean field velocities possess inflexion points and according to Rayleigh criterium for parallel flows, are unstable to transverse time-dependent perturbations. The inflexion point is located in the inner region whose extent depends on the inner rotation speed. This may explain the dependence of turbulent fraction upon Ri.

The occurrence of turbulent bursts in the laminar pattern of interpenetrating spirals is a subcritical bifurcation, therefore it can be described by the fifth order Landau equation which is known to exhibit, two coexisting states in a given range of values of the control parameter [18,22]. For small values of the control parameter, the turbulent state is metastable and decays after a short time into the absorbing laminar phase, while for large values, the laminar state becomes metastable and decays into a turbulent state. This is the scenario of spatio-temporal intermittency observed in extended systems such as Taylor-Dean system [8] and Rayleigh-Bénard convection [9,10]. In the counter-rotating Couette-Taylor system, as the control parameter is increased, the growth of turbulent bursts leads to a pattern in which there is a stable coexistence of turbulent and laminar spirals in a finite range of values of Ri. No invasion of turbulent state into laminar phase nor a decay of turbulent state is observed. The average axial width of turbulent spirals and that of laminar domains remain constant as Ri is increased. Moreover, histograms of the size of laminar domains have shown only the so called *algebraic regime*, no exponential decay of the size of laminar domains has been observed in that case [20]. In order to explain this coexistence of two stable state in time and for a finite range of Ri, Hayot and Pomeau [22] conjectured the existence of a mean flow induced by the turbulent fluctuations and added to the Ginzburg-Landau equation for the amplitude A a nonlocal term $I \sim \frac{1}{L}\int_0^L |A|^2 \mathrm{d}x$ which represents the mean energy of the perturbation in the system [22]. The resulting equation reads:

$$\frac{\partial A}{\partial t} = \mu A + D\frac{\partial^2 A}{\partial x^2} + \beta(|A|^2 - I)A - \delta|A|^4 A$$

where μ is the relative distance from the onset of the featureless turbulence, D is a diffusion coefficient, the Landau non linear constants $\beta > 0$ and $\delta > 0$. Numerical simulations of this equation [22] have shown that the expansion of turbulent domains saturates in time and in size leading to a stable turbulent spiral coexisting with a laminar one. Therefore the constant average width of the turbulent spiral with respect to Ri measured in our experiment (Fig. 8) is consistent with this numerical result. A similar model using a pressure gradient was developed by Stassinopoulos *et al.* [27] in order to describe periodic states of intermittency observed in pipe flows.

5 Conclusion

We have measured the turbulent fraction for turbulent states (bursts and spirals) in the Couette-Taylor system and found that it increases with angular velocities of both the cylinders. The axial velocity of turbulent spirals is a linear function of the outer cylinder rotation velocity. The wavelength of turbulent-laminar spirals does not depend upon the inner cylinder angular velocity but on that of the outer cylinder. Therefore, the two counter-rotating cylinders play a non symmetric role in the generation of intermittency states (turbulent bursts and turbulent spirals).

The author would like to thank Arnaud Mura, Patrice Laure and Olivier Dauchot for interesting discussions during the work. A. Goharzadeh benefits from a MENRT scholarship.

References

1. D.J. Tritton, *Physical Fluid Dynamics* (Oxford University press, Oxford, 1989).
2. I.J. Wygnanski, F. Champagne, J. Fluid Mech. **59**, 281 (1973).
3. D.R. Carlson, S.E. Widnall, M.F. Peters, J. Fluid Mech. **121**, 487 (1982).
4. M. Nishioka, M. Asai, J. Fluid Mech. **150**, 441 (1985).
5. C.D. Andereck, S.S. Liu, H.L. Swinney, J. Fluid Mech. **164**, 155 (1986).
6. D Coles, J. Fluid Mech. **21**, 385 (1965).
7. C. Van Atta, J. Fluid Mech. **25**, 495 (1966).
8. M. Degen, I. Mutabazi, C.D. Andereck, Phys. Rev. E **53**, 3495 (1996).

9. S. Ciliberto, P. Bigazzi, Phys. Rev. Lett. **60**, 286 (1988).
10. F. Daviaud, M. Bonetti, M. Dubois, Phys. Rev. A **42**, 3388 (1990).
11. H. Willaime, O. Cardoso, P. Tabeling, Phys. Rev. E **48**, 288 (1993).
12. K. Kaneko, Prog. Theo. Phys. **74**, 1033 (1985).
13. H. Chate, P. Manneville, Phys. Rev. Lett. **58**, 112 (1987).
14. F. Daviaud, J. Lega, P. Bergé, P. Coullet, M. Dubois, Physica D **55**, 287 (1992).
15. R.J. Deissler, J. Stat. Phys. **40**, 371 (1985).
16. H. Chate, Nonlinearity **7**, 185 (1994).
17. H. Chate, P. Manneville, Europhys. Lett. **6**, 591 (1988). See also H. Chate, P. Manneville, J. Stat. Phys. **56**, 357 (1989).
18. Y. Pomeau, Physica D **23**, 3 (1986). See also P. Manneville, *Structures Dissipatives et Turbulence* (Aléa Saclay, 1991).
19. K. Coughlin, P.S. Marcus, Phys. Rev. Lett. **77**, 2214 (1996).
20. P.W. Colovas, C.D. Andereck, Phys. Rev. E **55**, 2736 (1997).
21. J.J. Hegseth, C.D. Andereck, F. Hayot, Y. Pomeau, Phys. Rev. Lett. **62**, 257 (1989).
22. F. Hayot, Y. Pomeau, Phys. Rev. E **50**, 2019 (1994).
23. G.B. Schubauer, P.S. Klebanoff, *NACA TN-3489*, (1955). See also H.W. Emmons, J. Aero. Sci. **18**, 490 (1951) or M. Van Dyke, *An Album of Fluid Motion* (The Parabolic Press, Stanford, California, 1982).
24. H. Litschke, K.G. Roesner, Exp. Fluids **24** , 201 (1998).
25. A. Prigent, O. Dauchot, in *Rencontres du Non Linéaire*, edited by Y. Pomeau, R. Ribotta (IHP-Paris, 2000), p. 83.
26. P. Laure, *private communication.*
27. D. Stassinopoulos, J. Zhang, P. Alström, M.T. Levinsen, Phys. Rev. E **50**, 1189 (1994).